



## Crystallographic direction dependence of direct current field induced strain and phase transitions in Na<sub>0.5</sub>Bi<sub>0.5</sub>TiO<sub>3</sub>-x%BaTiO<sub>3</sub> single crystals near the morphotropic phase boundary

Chengtao Luo, Wenwei Ge, Qinhui Zhang, Jiefang Li, Haosu Luo, and D. Viehland

Citation: [Applied Physics Letters](#) **101**, 141912 (2012); doi: 10.1063/1.4757877

View online: <http://dx.doi.org/10.1063/1.4757877>

View Table of Contents: <http://scitation.aip.org/content/aip/journal/apl/101/14?ver=pdfcov>

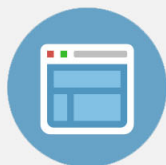
Published by the [AIP Publishing](#)

---



## Re-register for Table of Content Alerts

Create a profile.



Sign up today!



# Crystallographic direction dependence of direct current field induced strain and phase transitions in $\text{Na}_{0.5}\text{Bi}_{0.5}\text{TiO}_3$ - $x\%$ $\text{BaTiO}_3$ single crystals near the morphotropic phase boundary

Chengtao Luo,<sup>1</sup> Wenwei Ge,<sup>1,a)</sup> Qinhui Zhang,<sup>2</sup> Jiefang Li,<sup>1</sup> Haosu Luo,<sup>2</sup> and D. Viehland<sup>1</sup>

<sup>1</sup>Department of Materials Science and Engineering, Virginia Tech, Blacksburg, Virginia 24061, USA

<sup>2</sup>Shanghai Institute of Ceramics, Chinese Academy of Sciences, Shanghai 201800, China

(Received 7 May 2012; accepted 24 September 2012; published online 5 October 2012)

The crystallographic dependence of the DC electric (E) field induced strain and phase transition in  $\text{Na}_{0.5}\text{Bi}_{0.5}\text{TiO}_3$ -5.6% $\text{BaTiO}_3$  (NBT-5.6%BT) single crystals has been investigated. An induced transition between pseudocubic and tetragonal structures was observed under  $E = 10$  kV/cm for fields applied along the  $\langle 001 \rangle$  direction, whereas an induced transition between pseudocubic and rhombohedral structures was observed when the E-field was applied along  $\langle 111 \rangle$ . Our results show near the morphotropic phase boundary that the phase stability of NBT- $x\%$ BT is dependent on the crystallographic direction along which E was applied. © 2012 American Institute of Physics. [<http://dx.doi.org/10.1063/1.4757877>]

Ferroelectrics with large field induced strains are important for high performance piezoelectric actuators. Solid solutions of  $\text{Na}_{0.5}\text{Bi}_{0.5}\text{TiO}_3$ - $x\%$  $\text{BaTiO}_3$  (abbreviated as NBT- $x\%$ BT) are potentially important lead-free piezoelectric systems, as they have a rhombohedral (R) to tetragonal (T) phase transition at a morphotropic phase boundary (MPB) near  $6 < x < 8$ .<sup>1,2</sup> Large field induced strains of  $\sim 0.45\%$  have been reported for NBT-based materials: i.e., NBT- $x\%$ BT<sup>3</sup> and NBT- $x\%$ BT- $y\%$  $\text{K}_{0.5}\text{Na}_{0.5}\text{NbO}_3$  (NBT- $x\%$ BT- $y\%$ KNN),<sup>4,5</sup> near a so-called depolarization temperature ( $T_d$ ) below which notable frequency dispersion of the dielectric constant was found.

The structural origin of the large strain in NBT- $x\%$ BT based materials was recently studied using *in-situ* x-ray and neutron diffraction.<sup>6-9</sup> Based on the splitting of the pseudocubic (200) reflection of NBT-7%BT ceramics under E-field, Daniels *et al.*<sup>6,7</sup> proposed that the combination of an E-field induced phase transformation from pseudocubic to tetragonal (T) structures, domain texture, and anisotropic lattice strains are responsible for the large induced strain. However, *in-situ* neutron diffraction studies have shown that large E-field induced strains in NBT-6%BT-2%KNN<sup>8</sup> and NBT-6%BT<sup>9</sup> ceramics are accompanied by a change of the oxygen octahedral tilt system from  $a^0a^0c^+$  (P4bm) to  $a^-a^-a^-$  (R3c) following the Glazer notation.<sup>10</sup> Subsequently, an E-field induced T (P4bm)  $\rightarrow$  rhombohedral (R, R3c) transformation was proposed to be responsible for the large strain, contradictory to Daniels' results.<sup>6,7</sup> However, there remains no explanation concerning this contradiction. Considering that the proper understanding of the correlation between structure and properties is crucial in developing new materials, identification of the structural origin of the large induced strain in NBT- $x\%$ BT could be important in the development of lead-free piezoelectric systems with electromechanical properties approaching that of Pb-based ones.<sup>11</sup>

Here, we report the crystallographic dependence of DC field induced phase transitions in  $\text{Na}_{0.5}\text{Bi}_{0.5}\text{TiO}_3$ -

5.6% $\text{BaTiO}_3$  single crystals. An induced pseudocubic  $\rightarrow$  T transformation was observed for  $E//\langle 001 \rangle$ , whereas an induced pseudocubic  $\rightarrow$  R transformation was observed for  $E//\langle 111 \rangle$ .

Single crystals of NBT- $x\%$ BT were grown by a top-seeded solution growth method.<sup>12</sup> The concentrations of Ba in the as-grown condition were determined by inductively coupled plasma atomic emission spectrometry (ICP-AES) to be 5.6 at. %. Pseudocubic  $\langle 001 \rangle$  and  $\langle 111 \rangle$  oriented NBT-5.6%BT crystal wafers with dimensions of  $2 \times 2 \times 0.4$  mm<sup>3</sup> were cut from the boule, and subsequently electroded on both surfaces with gold. Temperature dependent dielectric constant measurements were performed using a LCR meter (HP 4284 A) under zero-field heating conditions in the temperature range of 30 °C to 600 °C. Unipolar strain ( $\epsilon$ -E) hysteresis loops were measured at a frequency of 1 Hz, using a linear variable differential transducer (LVDT) driven by a lock-in amplifier (Stanford Research, SR850) in the temperature range from 25 °C to 180 °C. Field dependent (200), (220), and (222) line and area scans were taken at various temperatures with increasing E-field between 0 and 20 kV/cm. These studies were done using a Philips MPD high-resolution x-ray diffraction system, equipped with a two bounce hybrid monochromator, an open three-circle Eulerian cradle, and a domed hot-stage. A Ge (220)-cut crystal was used as an analyzer, which had an angular resolution of 0.0068°. The x-ray wavelength was that of  $\text{CuK}_\alpha = 1.5406$  Å, and the x-ray generator was operated at 45 kV and 40 mA.

Figures 1(a) and 1(b) show  $\epsilon$ -E curves for NBT-5.6%BT measured at various temperatures under a maximum DC electric field of  $E = 20$  kV/cm applied along [001] and [111]. For the [001] orientation, the  $\epsilon$ -E curves were nearly linear and anhysteretic below 130 °C. The maximum strain at 25 °C was  $\epsilon_{\text{max}} = 0.09\%$ . With increasing temperature,  $\epsilon_{\text{max}}$  increased modestly to 0.12% at 80 °C. At 130 °C, a large increase in  $\epsilon$  was found near  $E = 8$  kV/cm, reaching values of  $\epsilon_{\text{max}} = 0.60\%$  under  $E = 20$  kV/cm. With further increase of temperature to 150 °C,  $\epsilon_{\text{max}}$  decreased to  $\sim 0.45\%$ . Strong hysteresis was observed for the  $\epsilon$ -E curves at 130 °C and

<sup>a)</sup>Electronic mail: wenweige@vt.edu.

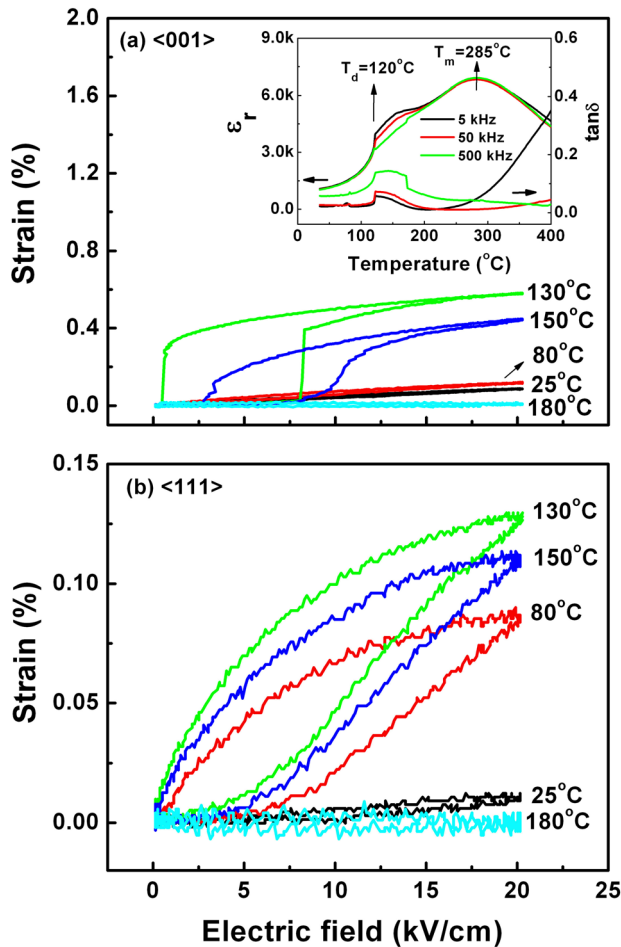


FIG. 1. Unipolar E-field dependent strain curves measured along (a) [001] and (b) [111] under 20 kV/cm at various temperatures for NBT-5.6%BT. The inset of (a) shows the temperature dependence of the dielectric constant  $\epsilon_r$  and loss factor  $\tan\delta$  for NBT-5.6%BT measured at frequencies of 5 kHz, 50 kHz, and 500 kHz.

150 °C. At 180 °C, no significant induced strains were found even for  $E = 20$  kV/cm. For [111] oriented crystals, the  $\epsilon$ -E curves were nearly linear and anhysteretic at 25 °C. However, strongly hysteretic  $\epsilon$ -E curves were observed above 80 °C. The value of  $\epsilon_{\max}$  was 0.01% at 25 °C and increased by a factor of 9 to 0.09% at 80 °C. The largest value for  $\epsilon_{\max}$  was 0.13% which was obtained at 130 °C, which then decreased to 0.11% on heating to 150 °C. Again, at 180 °C, significant induced strains were not found for  $E//[111]$ .

A comparison of the normalized strain  $\epsilon_{\max}/E_{\max}$ , which is an important parameter for actuator applications, for NBT-5.6%BT single crystals and previously reported data for KNN-modified NBT- $x$ %BT ceramics<sup>4,5</sup> is given in Table I. This table reveals that (1) the value of  $\epsilon_{\max}/E_{\max}$  for NBT-5.6%BT crystals along [001] are much higher than that along [111]; and (2) the value of  $\epsilon_{\max}/E_{\max}$  along both [001] and [111] are significantly increased at 130 °C, near the depolarization temperature ( $T_d$ ) above which the dielectric constant became notably frequency dispersive (see inset of Fig. 1(a)). The value of  $T_d$  for NBT- $x$ %BT compositions near the MPB was shifted to lower temperatures by doping with KNN, which also enhanced the electrically induced strain. On doping NBT-6%BT with 1 mol. % KNN, the value of  $\epsilon_{\max}/E_{\max}$  increased from 240 pm/V to 310 pm/V at 25 °C, while  $T_d$

TABLE I. The comparison of  $\epsilon_{\max}/E_{\max}$  for NBT-5.6%BT crystals with previously reported data for KNN-modified NBT-6%BT ceramics.

Material	$\epsilon_{\max}/E_{\max}$ (pm/V)	Measured temperature ( °C)
$\langle 001 \rangle$ -oriented NBT-5.6%BT crystal	450	25
$\langle 111 \rangle$ -oriented NBT-5.6%BT crystal	50	25
$\langle 001 \rangle$ -oriented NBT-5.6%BT crystal	3000	130
$\langle 111 \rangle$ -oriented NBT-5.6%BT crystal	650	130
94NBT-6%BT ceramics	240	25
93NBT-6%BT-1%KNN ceramics	310	25
93NBT-6%BT-1%KNN ceramics	680	60
92NBT-6%BT-2%KNN ceramics	560	25

was decreased from 130 °C to 60 °C.<sup>5</sup> Similar to NBT-5.6%BT crystals (as shown in Fig. 1),  $\epsilon_{\max}/E_{\max}$  was previously reported to be increased to 680 pm/V near  $T_d$  (see Table I) for ceramics doped with 1 mol. % KNN.<sup>5</sup> With further increase of KNN content to 2 mol. %,  $T_d$  was shifted to room temperature and the value of  $\epsilon_{\max}/E_{\max}$  was increased to 560 pm/V at 25 °C. On the basis of temperature dependent P-E hysteresis measurements, Jo *et al.*<sup>5</sup> proposed that the presence of a nonpolar phase results in KNN-modified NBT-6%BT returning to its unpoled condition after removal of E, which in turn results in an enhancement of  $\epsilon_{\max}/E_{\max}$  near  $T_d$ . Previous structural investigations have given two different explanations for this enhancement of  $\epsilon_{\max}/E_{\max}$  near  $T_d$ : (1) pseudocubic  $\rightarrow$ T<sup>6,7</sup> and (2) T ( $P4bm$ )  $\rightarrow$ R ( $R3c$ )<sup>8,9</sup> transformations. However, in Table I, it can be seen that the enhancement of  $\epsilon_{\max}/E_{\max}$  near  $T_d$  for NBT-5.6%BT crystals is dependent on the crystallographic direction along which E is applied: please note this enhancement was more pronounced for crystals relative to ceramics. Thus, it is important to further identify the mechanism of this enhancement in  $\epsilon_{\max}/E_{\max}$  for crystals. Such an understanding could be important to lead-free piezoelectrics with giant strains for actuator applications.

Figures 2(a) and 2(b) show  $\omega$ - $2\theta$  area scans at 130 °C for NBT-5.6%BT crystals under  $E = 0$  kV/cm taken about (002)<sub>PC</sub> and (111)<sub>PC</sub>. A single sharp peak can be seen along each zone. No information concerning oxygen octahedral tilt reflections was obtained, as such reflections were too weak to be measured using a high-resolution lab diffractometer. Prior transmission electron microscopy (TEM) studies have revealed the coexistence of ferroelectric polar nanoregions of  $R3c$  and  $P4bm$  symmetry in NBT- $x$ %BT near the MPB<sup>13,14</sup> but the average long range symmetry may be cubic.<sup>15</sup> Thus, the phase structure of NBT-5.6%BT for  $E = 0$  in the present study is referred to pseudo-cubic, as previously reported.<sup>6,7,9</sup> The pseudo-cubic lattice parameters were  $a = 3.909 \pm 0.002$  Å for  $E = 0$  kV/cm at 25 °C.

Two different E-field induced transformations were then observed for NBT-5.6%BT crystals under E applied along [001] and [111] at 130 °C. For  $E//[001]$ , the (200) reflection in the  $\omega$ - $2\theta$  area scan for  $E = 10$  kV/cm split along both the  $2\theta$  and  $\omega$  axes (see Fig. 2(c)); whereas, the (111) reflection split only along the  $\omega$  axis in the  $\omega$ - $2\theta$  area scan (see Fig. 2(d)). The  $2\theta$  positions of these peaks were found at  $2\theta = 46.073^\circ$ ,  $46.662^\circ$ , and  $39.952^\circ$  for the (200) and (111) reflections. These results revealed two  $d$  spacings for the

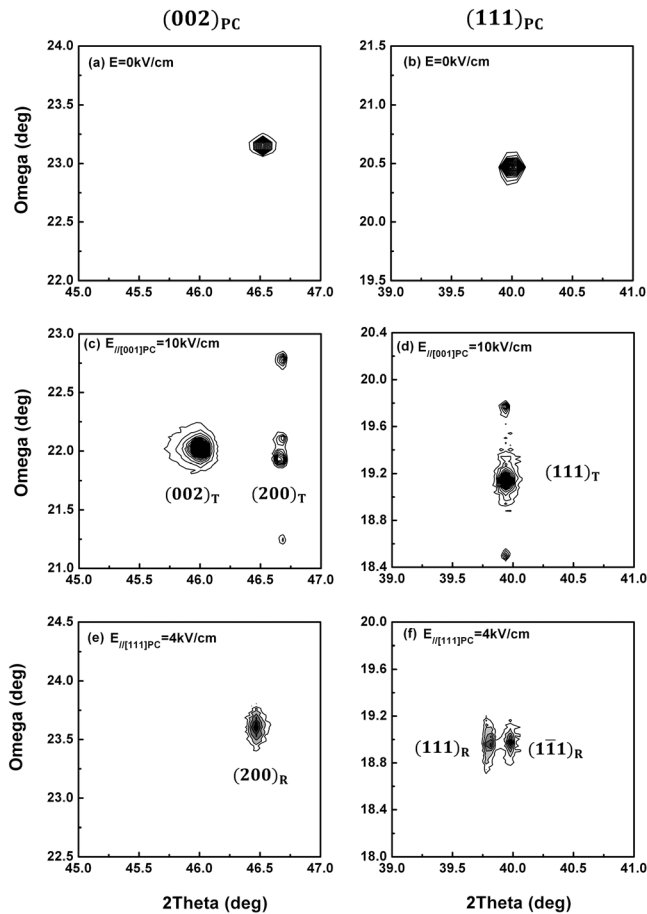


FIG. 2.  $\omega$ - $2\theta$  maps taken along the  $(002)_{PC}$  and  $(111)_{PC}$  zones at  $130^\circ\text{C}$ : [(a) and (b)] under zero E, [(c) and (d)] under  $E//[001]_{PC} = 10\text{ kV/cm}$ , and [(e) and (f)] under  $E//[111]_{PC} = 4\text{ kV/cm}$ .

$(200)$  reflection and one  $d$  spacing for the  $(111)$  reflection according to the Bragg law, i.e.,  $2d_{hkl} \sin \theta_{hkl} = \lambda$ , where  $(hkl)$  is reflection indices. These results demonstrate an E-field induced pseudocubic  $\rightarrow$  T transition for  $E//[001]$  under  $10\text{ kV/cm}$ . The lattice parameters for the induced T phase were  $(a_c, c_t) = (3.890, 3.937) \pm 0.002 \text{ \AA}$ . Though the peaks split along  $\omega$  axis for the  $(200)_T$  and  $(111)_T$  reflections, these peaks are at the same  $2\theta$  positions. This indicated that these reflection peaks resulted from tilted domains having the same  $d$  spacings to release strain generated during E-field induced pseudocubic  $\rightarrow$  T transition. However, for  $E//[111]$ , a  $2\theta$  splitting was observed about the  $(111)$  reflection in the  $\omega$ - $2\theta$  for  $E = 4\text{ kV/cm}$  (see Fig. 2(f)), but no splitting was observed around the  $(200)$  (see Fig. 2(e)). These data demonstrate that an E-field induced pseudocubic  $\rightarrow$  R transition occurs under  $E//[111]$  for  $4\text{ kV/cm}$ . The lattice parameters of this induced R phase were  $(a_r, \alpha_r) = (3.908 \text{ \AA}, 89.78^\circ)$ .

Figures 3(a) and 3(b) show the E-field dependent lattice parameters at  $130^\circ\text{C}$  for E applied along  $[001]$  and  $[111]$  directions, respectively. For  $E//[001]$ , the lattice parameters of the pseudocubic structure increased with increasing field for  $E \leq 8\text{ kV/cm}$ . With increasing E to  $10\text{ kV/cm}$ , a tetragonal splitting of  $c/a = 1.012$  became apparent, demonstrating an induced phase transformation. Please note that the  $\epsilon$ -E curve for  $[001]$  at  $130^\circ\text{C}$  exhibited a jump at  $E \approx 8\text{ kV/cm}$  (see Fig. 1(a)), near which this induced pseudocubic  $\rightarrow$  T transition occurs. These data show that the enhancement of

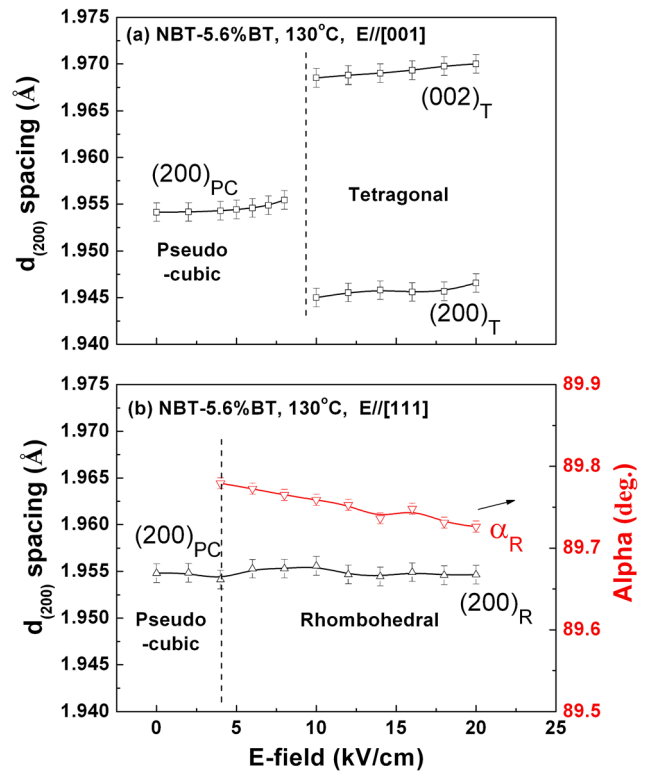


FIG. 3. Electric field dependent  $d$  spacing of  $(200)$  for NBT-5.6%BT at  $130^\circ\text{C}$  under (a)  $E//[001]$ , and (b)  $E//[111]$ .

$\epsilon_{\text{max}}/E_{\text{max}}$  near  $T_d$  for  $[001]$  oriented crystals is due to this induced transformation. For  $E//[111]$ , an obvious R distortion appeared with increasing field near  $E = 4\text{ kV/cm}$ , where the rhombohedral angle was  $\alpha_r = 89.78^\circ$ .

These structural results show that the E-field induced phase transformations in NBT-5.6%BT crystals are dependent on crystallographic direction along which E is applied: an induced pseudocubic  $\rightarrow$  T transition was observed near  $E = 10\text{ kV/cm}$  for  $E//[001]$ , whereas an induced pseudocubic  $\rightarrow$  R one was found for  $E//[111]$ . Although NBT- $x\%$ BT crystals for compositions close to the MPB have been found to be pseudocubic under zero field, transmission electron microscopy studies have revealed the coexistence of polar nano-regions with an  $a^0a^+c^+$  in-phase oxygen octahedral tilting ( $P4bm$  structure), and an  $a^-a^-c^-$  anti-phase oxygen octahedral tilting ( $R3c$  structure).<sup>14</sup> In the polar nano-regions with a  $P4bm$  structure, the  $\text{Na}^{1+}/\text{Bi}^{3+}$  and  $\text{Ti}^{4+}$  cations displace almost equally in opposite directions along the  $[001]_{PC}$ , resulting in the T ( $P4bm$ ) phase being only weakly polar.<sup>16</sup> In the polar nano-regions with a  $R3c$  structure, the displacement of the  $\text{Na}^{1+}/\text{Bi}^{3+}$  and  $\text{Ti}^{4+}$  cations are parallel along the  $[111]_{PC}$  axis.<sup>16</sup> The crystallographic dependence of the induced phase transformations can be attributed to the response of T and R polar nano-regions under E applied along their respective polar directions. Near the MPB, either R or T phases can be induced, depending on the direction along which E is applied, as the two phases are nearly thermodynamically degenerate.

The crystallographic orientation dependent E-field phase stability has previously been reported for PMN- $x\%$ PT near the MPB.<sup>17-19</sup> For PMN-30%PT single crystals, an E-field induced  $R \rightarrow$  Monoclinic A ( $Cm$ )  $\rightarrow$  Monoclinic C ( $Pm$ )  $\rightarrow$  T



phase transformation sequence was reported for E applied along [001],<sup>19</sup> whereas an E-field induced R → Monoclinic B (*Cm*) sequence was found for E applied along [111].<sup>18</sup> These low symmetry monoclinic phases allow the polarization vector to rotate within a plane under E giving rise to enhanced piezoelectric responses near the MPB.<sup>20</sup> Compared to PMN-x%PT, NBT-x%BT near its MPB has a unique feature which is that polar nano-regions with a<sup>0</sup>a<sup>0</sup>c<sup>+</sup> in-phase oxygen octahedral tilting (*P4bm* structure) and a<sup>-</sup>a<sup>-</sup>a<sup>-</sup> anti-phase oxygen octahedral tilting (*R3c* structure) coexist.<sup>14</sup> However, no low symmetry monoclinic phases and only T and R phases were induced from the initial pseudocubic one under E//[001] and E//[111] for NBT-5.6%BT crystals. These results indicate that both E-field induced pseudocubic → T and pseudocubic → R transitions make contributions to the enhanced strain properties in NBT-x%BT ceramics near the MPB compositions. However, the induced phases showed strong domain texture in ceramics with the polarization aligning preferentially parallel to the E-field.<sup>6,9</sup> Thus, only splitting of (002)/(200) peaks for the tetragonal distortion was detected in NBT-7%NBT<sup>6</sup> and NBT-x%BT-y%KNN<sup>7</sup> ceramics under the experiment configuration of scattering vectors parallel to the E-field in previous high-energy x-ray scattering experiments. The splitting of (111)/(1 $\bar{1}$ 1) peaks for the rhombohedral distortion in NBT-6%BT ceramics were reported at the angle of 30°–50° for the scattering vectors respect to the E-field,<sup>9</sup> which is consistent with the crystallographic orientation dependent E-field phase stability in NBT-5.6%BT single crystals reported here.

In summary, the crystallographic dependence of DC electric (E) field induced strains and phase transitions in Na<sub>0.5</sub>Bi<sub>0.5</sub>TiO<sub>3</sub>-5.6%BaTiO<sub>3</sub> single crystals were investigated. An induced transition between pseudocubic and T structures was observed under E = 10 kV/cm for E//[001], whereas an induced transition between pseudocubic and R structures was observed for E//[111]. Our results indicate that phase stability for compositions close to the MPB boundary is dependent on the direction along which E is applied.

This work was supported by the National Science Foundation (Materials World-Wide Network) DMR-0806592, by the Natural Science Foundation of China 50602047, by the Shanghai Municipal Government 08JC1420500, by the Innovation Fund of Shanghai Institute of Ceramics Y09ZC4140G, and by the Ministry of Science and Technology of China through 973 Program 2009CB623305.

- <sup>1</sup>T. Takenaka, K. Maruyama, and K. Sakata, *Jpn. J. Appl. Phys., Part 1* **30**(9B), 2236 (1991).
- <sup>2</sup>W. Jo, J. E. Daniels, J. L. Jones, X. Tan, P. A. Thomas, D. Damjanovic, and J. Rödel, *J. Appl. Phys.* **109**(1), 014110 (2011).
- <sup>3</sup>Y. M. Chiang, G. W. Farrey, and A. N. Soukhovjak, *Appl. Phys. Lett.* **73**(25), 3683 (1998).
- <sup>4</sup>S. T. Zhang, A. B. Kouna, E. Aulbach, H. Ehrenberg, and J. Rödel, *Appl. Phys. Lett.* **91**(11), 112906 (2007).
- <sup>5</sup>W. Jo, T. Granzow, E. Aulbach, J. Rödel, and D. Damjanovic, *J. Appl. Phys.* **105**(9), 094102 (2009).
- <sup>6</sup>J. E. Daniels, W. Jo, J. Rödel, and J. L. Jones, *Appl. Phys. Lett.* **95**(3), 032904 (2009).
- <sup>7</sup>J. E. Daniels, W. Jo, J. Rödel, V. Honkimaki, and J. L. Jones, *Acta Mater.* **58**(6), 2103 (2010).
- <sup>8</sup>M. Hinterstein, M. Knapp, M. Hölzel, W. Jo, A. Cervellino, H. Ehrenberg, and H. Fuess, *J. Appl. Crystallogr.* **43**(6), 1314 (2010).
- <sup>9</sup>H. Simons, J. Daniels, W. Jo, R. Dittmer, A. Studer, M. Avdeev, J. Rödel, and M. Hoffman, *Appl. Phys. Lett.* **98**(8), 082901 (2011).
- <sup>10</sup>A. Glazer, *Acta Crystallogr., Sect. B* **28**(11), 3384 (1972).
- <sup>11</sup>J. Rödel, W. Jo, K. T. P. Seifert, E. M. Anton, T. Granzow, and D. Damjanovic, *J. Am. Ceram. Soc.* **92**(6), 1153 (2009).
- <sup>12</sup>Q. H. Zhang, Y. Y. Zhang, F. F. Wang, Y. J. Wang, D. Lin, X. Y. Zhao, H. S. Luo, W. W. Ge, and D. Viehland, *Appl. Phys. Lett.* **95**(10), 102904 (2009).
- <sup>13</sup>W. Jo, S. Schaab, E. Sapper, L. A. Schmitt, H.-J. Kleebe, A. J. Bell, and J. Rödel, *J. Appl. Phys.* **110**(7), 074106 (2011).
- <sup>14</sup>J. Yao, N. Monsegue, M. Murayama, W. Leng, W. T. Reynolds, Q. Zhang, H. Luo, J. Li, W. Ge, and D. Viehland, *Appl. Phys. Lett.* **100**(1), 012901 (2012).
- <sup>15</sup>W. Jo, R. Dittmer, M. Acosta, J. Zang, C. Groh, E. Sapper, K. Wang, and J. Rödel, *J. Electroceram.* **29**, 71 (2012).
- <sup>16</sup>G. O. Jones and P. A. Thomas, *Acta Crystallogr. B* **58**, 168 (2002).
- <sup>17</sup>H. Cao, F. M. Bai, N. G. Wang, J. F. Li, D. Viehland, G. Y. Xu, and G. Shirane, *Phys. Rev. B* **72**(6), 064104 (2005).
- <sup>18</sup>H. Cao, J. F. Li, and D. Viehland, *J. Appl. Phys.* **100**(8), 084102 (2006).
- <sup>19</sup>F. M. Bai, N. G. Wang, J. F. Li, D. Viehland, P. M. Gehring, G. Y. Xu, and G. Shirane, *J. Appl. Phys.* **96**(3), 1620 (2004).
- <sup>20</sup>R. Guo, L. E. Cross, S. E. Park, B. Noheda, D. E. Cox, and G. Shirane, *Phys. Rev. Lett.* **84**(23), 5423 (2000).